Design and Implementation of High Dynamics Servo-Valve Driver for Electro-hydraulic Actuator in Legged Robot's Applications

Ghiath Abdulmalek, Anas Ammounah, Naïma Aït Oufroukh, Samer Alfayad, Saïd Mammar

Design and Implementation of High Dynamics Servo-Valve Driver for Electro-hydraulic Actuator in Legged Robot's Applications

Ghiath Abdulmalek
IBISC Lab
Univ Evry, Paris-Saclay University
Évry, France
giath.abdulmalek@univ-every.fr

Anas Ammounah
IBISC Lab
Univ Evry, Paris-Saclay University
Évry, France
anas.ammounah@univ-every.fr

Naïma Ait Oufroukh
IBISC Lab
Univ Evry, Paris-Saclay
*University´*Evry, France
naima.aitoufroukh@univ-evry.frfr

Samer Alfayad
IBISC Lab
Univ Evry, Paris-Saclay University
Évry, France
samer.alfayad@univ-every.fr

Saïd Mammar
IBISC Lab
Univ Evry, Paris-Saclay University
Évry, France
said.mammar@univ-every.fr

***Abstract*—Electro-Hydraulic Actuator (EHA) is widely used in many applications, such as humanoid robotics, rehabilitation devices, prosthetics, aeronautics, and industrial actuators. In robotics and legged robots development, high dynamics and wide bandwidth are major issues. The electro-hydraulic servo-valve (EHSV) plays a vital role in controlling electrohydraulic actuators due to the high bandwidth as a main advantage compared to the conventional electro-hydraulic proportional valves. To take advantage of this criteria, the components of the driving system should be well designed in respect of the desired dynamic behavior. Certain EHSVs have unique electrical characteristics that make them difficult to drive. This paper presents a new topology electronic driver to enhance the dynamic characteristics of the EHSV-based actuation system. A theoretical study has been conducted for the driver, and the design is well verified using the Simscape tool (hydraulics, electrical and mechanical) in Simulink MATLAB. Finally, experimental results are obtained on a laboratory hydraulic system test bench.**

***Index Terms*—High Bandwidth Actuators, Dynamic Driver, Servo-valve, Modelling, Current Controller, Torque motor, Electro-Hydraulic Servo-valve (EHSV), Servo-Electro Hydraulic Actuator (SEHA)**

I. Introduction

One of the major issues in robotics research is creating an actuator system for high dynamic-legged robots. The main criterion needed for highly dynamic tasks is the wide bandwidth of the actuation system [1] [2] [3]. Electric actuators for legged robots can achieve very high bandwidth. These dynamics have been shown in LOLA humanoid robot by achieving 240 Hz for the closed loop joint controller during the typical walking sequence. The servo electronic driver from ELMO Motion Control has been used for each joint. It allows a high sampling rate for the feedback [4]. Pneumatic actuators cannot provide high bandwidth compared to electric and hydraulic actuators. This is because of the high compressibility of the air-fluid [5]. Although, some pneumatically actuated robots and bio-inspired muscles have been developed to emulate human muscles [6] [7]. Hydraulic actuation is popular in the industry for heavy-duty applications but is not very common in robotics. Although hydraulic actuation has shown an ability for high dynamics performance, such as the ATLAS robot [8], SARCOS CB robot [9] and HyQ2Max [10]. ATLAS robot is the most advanced humanoid robot; it has impressive dynamic behaviour. Unfortunately, very little information is published about the hardware of the robot. Different hydraulic valves are available like proportional valves, piezo servo-valves, pipejet, and flapper-nozzle servo-valves. Proportional valves are more affordable than servo-valves [11]. Some hydraulically-actuated robots have used proportional valves, like the lower limb exoskeleton from Virginia Tech [12] and the earlier version of HyQ robot [13]. These examples didn't show high dynamics performance due to the limited bandwidth of the proportional valve, which doesn't exceed some tens of Hz [14].

Flapper-nozzle servo-valves and pipejet servo-valves are two similar types of valves. They provide fast response and high accuracy in a small size [15]. Both of them are two-stage servo-valves. The first stage is an electrical torque motor.

The Piezoelectric valves are direct one-stage valves. It uses

Piezoelectric actuators PEAs instead of the torque motor in the flapper-nozzle and pipejet servo-valves [11]. The PEAs use the inverse effect of the piezo material: it deforms mechanically when applying excitation voltage to it. The material reacts very quickly, which allows obtaining a very high bandwidth for the servo-valve to achieve the range of 1 kHz [16].

The deformation of the piezoelectric material is relatively small (some micrometers). Therefore, most PEAs adopt complex mechanical amplification to increase stroke. As a result, the piezoelectric servo-valves need special electronic drivers, and the size of such drivers is quite extensive [16].

In our research, we focus on hydraulic actuation by using the flapper-nozzle servo-valves. In the challenge of increasing the response dynamics of the servo-valve-based electro-hydraulic actuation, many approaches are proposed in the literature. One of them suggests using the flow-forward compensation principle. A double valve-control scheme has been used [17]. Another approach is based on the use of a magnetic fluid in the torque motor of the servo-valve. It has been shown that it can increase the responsivity of the torque motor [18].

In our approach, the electrical characteristics of the torque motor of the Moog 30-series and E024-series have been studied, and the electronic driver has been investigated.

The remainder of the paper is organized as follows. Section II is dedicated to the modelling problem of the servo-valve. Section III presents the proposed solution, while Section IV provides the simulation results. Implementation results are detailed in Section V, while Section VI warps up the paper.

II. Problematic of dynamic model of MOOG3 series servo-valve

A. Principle of Electro-Hydraulic Servo-Valve

An electro-hydraulic servo-valve is a type of valve used in hydraulic control systems to regulate the flow and pressure of the fluid. There are many servo-valves, but the most common and efficient type is the flapper nozzle servo-valve; the valve uses a flapper and nozzle mechanism, along with a feedback spring, to control the flow of hydraulic fluid and maintain the desired position or velocity of the actuator [16]. Another critical component of the servo-valve is the torque motor coupled with the flapper, that causes it to move and change the flow in the nozzle workflow of the servo-valve is as follows:

1) Electrical input: The electric input of the servo-valve is the current flow through the torque motor's coils. The current will activate the coils generating a magnetic field. This field acts on a magnetic armature connected to the pivoting arm, causing it to move in a specific direction.
2) Flapper and nozzle mechanism: The nozzle is a small opening through which the fluid flows, and the flapper is a thin, flexible piece of metal attached to a pivoting arm. The current signal controls the position of a flapper within the servo-valve. The position of the flapper determines the size of the opening between the nozzles and, therefore, the flow of hydraulic fluid through the valve (internal flow).

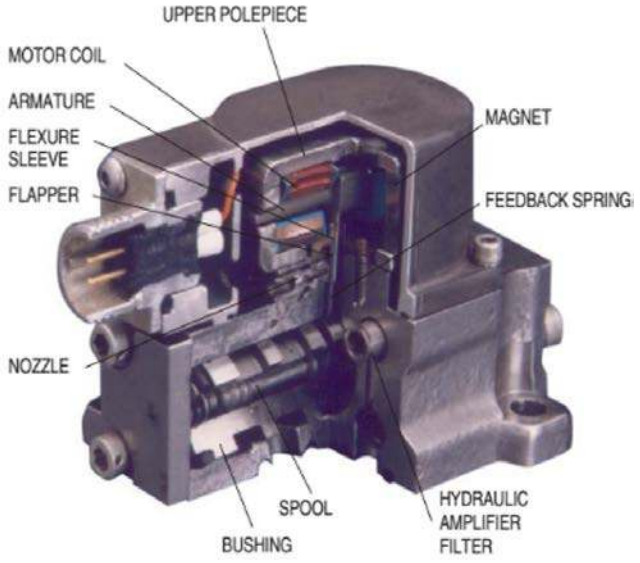

Fig. 1. Servo-valve typical design [22]

3) Main Spool Movement: The valve has a housing with an inlet and outlet port for hydraulic fluid and a spool mounted inside the housing. This spool has several lands (also called spool positions) that can block or allow fluid flow through the valve (from inlet to outlet and vice versa), depending on its position. The flow from the previous stage(flapper-nozzle) will generate a differential pressure on the main spool and make it move.
4) Feedback spring: The hydraulic fluid flows through the valve and is directed to the actuator. At the same time, the position of the flapper is also controlled by a feedback spring. The feedback spring provides a force that opposes the force of the electrical input signal and helps to hold the flapper in position.
5) Actuator control: The position of the flapper and the size of the opening between the nozzles determine the flow of the hydraulic fluid to the actuator, which then moves to the desired position or velocity. As the actuator moves, it sends a feedback signal back to the control system, which can be used to adjust the electrical input signal and maintain the desired position or velocity.

The typical operational parts of the studied servo-valve and the principle of operation are shown in Figures 1 and 2.

The feedback spring is connected to the hydraulic spool and provides a force that opposes the force of the electrical signal. This allows the spool to be precisely positioned and held in place by balancing forces between the electrical signal and the spring.

The feedback spring is typically calibrated to provide a specific level of resistance to the movement of the spool. The calibration of the spring is critical for the performance of the servo-valve, as it determines the sensitivity and stability of the valve's response to the electrical input signal.

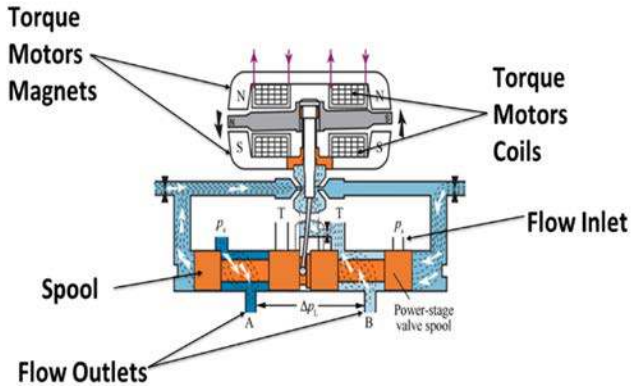

Fig. 2. EHSV working principle

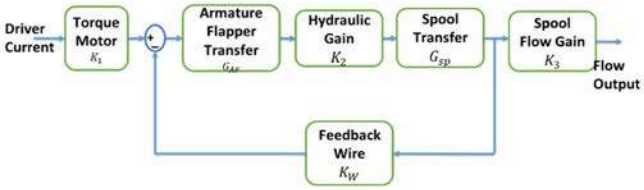

Fig. 3. Servo-valve Dynamic Model Block Diagram [5]

In conclusion, the EHSV consists mainly of two stages; the first stage is a torque motor with a flapper nozzle, and the second stage is a standard four-spool valve [19].

B. Dynamic Model Problem

Although the simplicity of its working principle (as explained above), the servo-valve is considered as a very complex system when we are trying to derive a control model because three domains of science are concerned in this system Mechanics, Hydraulics, and Electrics.

Many works have been done to derive a good model representing the servo-valve [20], [21].

Although much work is done for EHSV modelling, they all start with the electric current as input for such a system, as shown in Figure 3[22], which supposes the ideal behaviour of the torque motor and ignores the current dynamics caused by the high values of the motor inductance and resistor.

To better explain this problem, let's consider the simplified servo-valve block diagram shown in Fig. 3 with parameters given in Table II. If we keep the torque motor as just a gain, we can write the following transfer functions:

$$G_{AF}(s) = \frac{\frac{1}{K_f}}{1 + 2\xi\frac{s}{\omega_n} + \frac{s^2}{\omega_n^2}} \tag{1}$$

$$G_{sp}(p) = \frac{1}{As} \tag{2}$$

Considering the control block diagram of Fig. 3 and the equations 1 and 2, we can express the current (in mA) to flow (in $m^3/\sec$) transfer function as in equation 3:

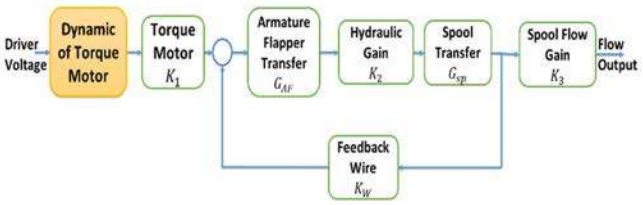

Fig. 4. Servo-valve Model considering the electric current Dynamic

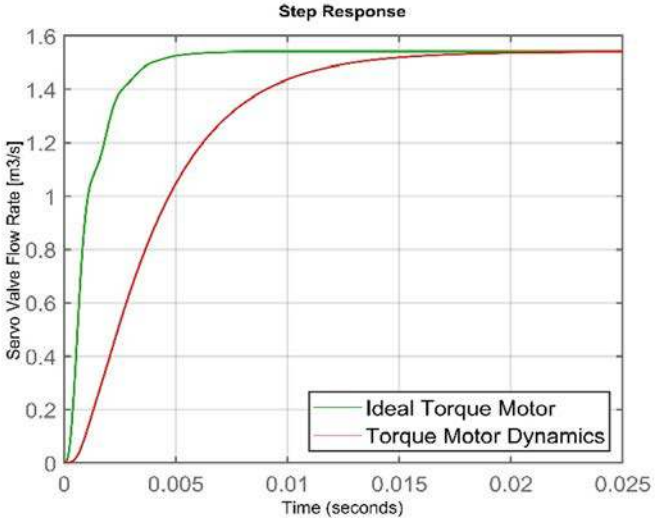

Fig. 5. Servo-valve Step Response (Green: Ideal Torque Motor, Red: Current Dynamic of the Torque motor is considered)

$$\frac{Q_v}{i} = \frac{\alpha}{\frac{A}{\omega_n^2}s^3 + \frac{2A\xi}{\omega_n}s^2 + As + \beta} \tag{3}$$

where $\alpha = \frac{K_1 K_2 K_3}{K_f}$ and $\beta = \frac{K_w K_2}{K_f}$.

Now, if we consider the current dynamics of the torque motor and add it to the control block diagram, as shown in Fig. 4, we can obtain the following transfer function.

$$\frac{Q_v(s)}{I(s)} = \frac{\alpha}{\frac{A}{\omega_n^2}s^3 + \frac{2A\xi}{\omega_n}s^2 + As + \beta}\frac{a_i}{1 + b_i s} \tag{4}$$

where $a_i = \frac{1}{R}$ and $b_i = \frac{L}{R}$.

Simulating the two transfer functions given is equations 3 and 4 with the same step input we get the result shown in Fig. 5. We notice clearly the high impact the dynamics of the torque motor on the servo-valve dynamic behaviour, where the settling time in the ideal torque motor case (the green curve) and for the case where the torque motor dynamic is considered (the red curve) $T_{Torque_s} = 10.8ms$ which is three times greater than the ideal case.

III. Proposed Solution

Considering the high impact of the current dynamics of the torque motor on the total EHSV system settling time which directly affects the dynamics of the robot's movement, we propose a new dynamic driver topology to overcome this

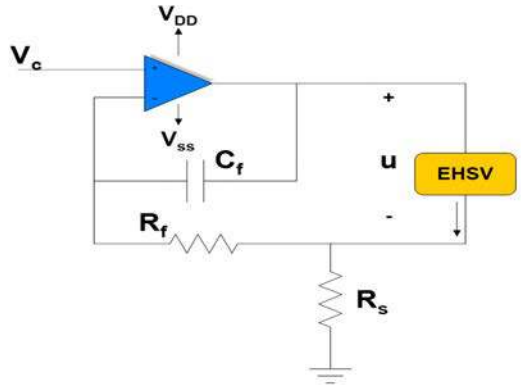

Fig. 6. High Dynamic Driver Proposed Schematic

problem and enhance the current dynamics of the torque motor, hence improving the total EHSV system's dynamics.

A. Proposed high dynamic driver

Fig. 6 shows the schematic of our proposed high dynamic driver, with $V_{DD} = 72V$ and $V_{SS} = -72V$.

1) Linear analysis of the driver: Analyzing the driver circuit linearly, supposing that $R \ll R_f$, we find that the output of the driver can be described by equation 5.

$$u = K_i \int (i_{ref} - i) + K_p(i_{ref} - i) \tag{5}$$

where $K_p = R_s$, $K_i = \frac{R_s}{R_f C_f}$ and $i_{ref} = \frac{v_c}{R_s}$.

Applying Laplace transform to equation 5 we got the equation 6

$$U(s) = \left(K_p + \frac{K_i}{s}\right) E(s) \tag{6}$$

where $E(s) = I_{ref}(s) - I(s)$ is the Laplace transform of the error.

2) Nonlinear analysis of the Driver: Saturation effects occur when any part of a feedback control system reaches a physical limit. And this is exactly what happens with an operational amplifier where the output voltage is limited to a value near the supply voltage. Since our current driver is established by means of operational amplifier, then we have the saturation effect, which could be expressed as:

$$V_0 = \begin{cases} +V_{sat} & if \quad V_{in^+} > V_{in^-} \\ -V_{sat} & if \quad V_{in^+} < V_{in^-} \end{cases} \tag{7}$$

In fact, the saturation effect of our driver will appear in the transient state where the speed change in the current is needed, as we will see in the simulation.

IV. Simulation Results

A. Current Control Loop – Inner Loop

To validate the dynamic behavior the proposed driver topology, we build a hydraulic cylinder system with mechanical load and with the proposed servo-valve model in Simscape

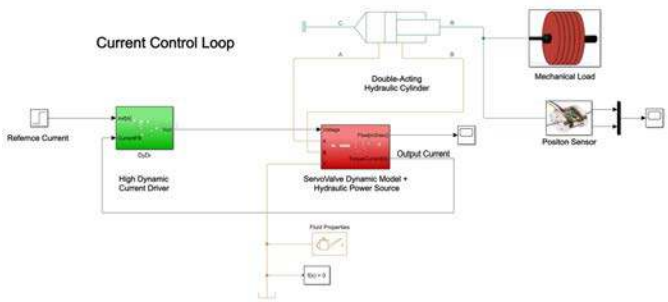

Fig. 7. Simscape simulation for the Hydraulic System, Servo-valve and Driver

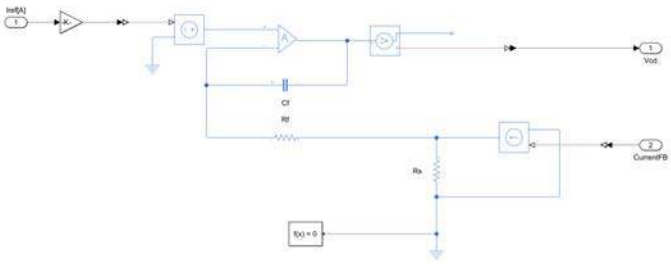

Fig. 8. Driver Circuit in SimElectrical

toolbox (Simhydraulics, Simmechanics) / MATLAB Simulink (Fig. 7).

The driver circuit is itself built using the Matlab SimElectrical toolbox and limited bandwidth OP-AMP with ±72 Volt as rail supply Fig. 8. As shown in (Fig. 9), the driver output is the OP-AMP voltage saturation $V_{DD} = 72V$ for the transient phase where the error between the desired current value and actual current is very high, but when the actual current gets close to the desired value we see clearly the linear behaviour of the driver.

B. Double Control Loop – Flow (Outer) and Current (Inner)

To verify the enhancement impact of our driver on the flow control loop, we simulate the flow control loop using a PID controller, as shown in Fig. 10.

Our main objective here is to examine the servo-valve flow-settling time, so we did not optimize the PID parameter to

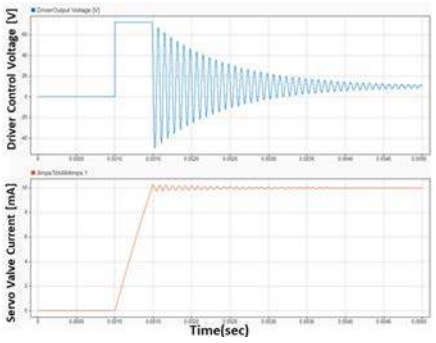

Fig. 9. Current Dynamic (Down-Orange) and Driver Output Voltage (Up-Blue)

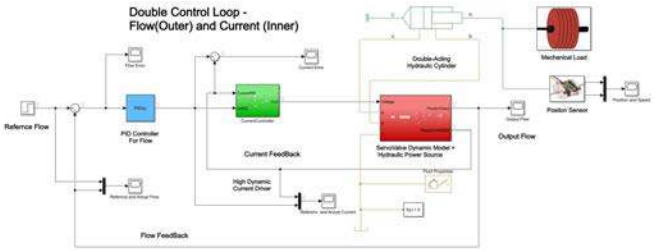

Fig. 10. Flow Control Loop (Outer) and Current Control Loop (Inner) in Simulink

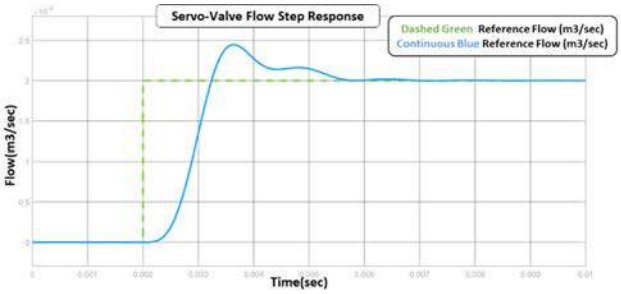

Fig. 11. Flow Step Response with High Dynamic Current Driver(181 % speed enhancement)

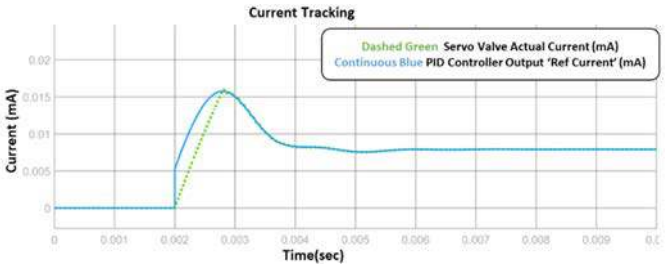

Fig. 13. Dynamic Driver Current Tracking

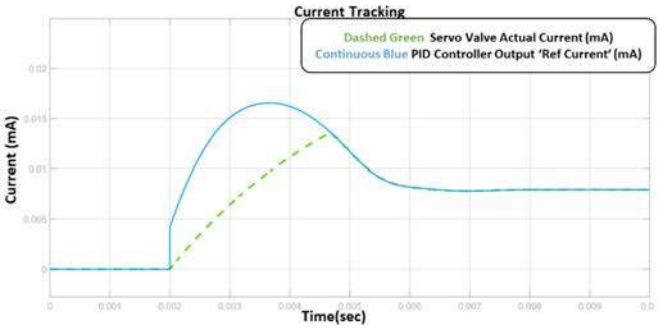

Fig. 14. Low Voltage Driver Current Tracking

obtain the fastest possible response, but we tuned the PID parameter to have acceptable performance in order just to compare the two cases:

1) The settling time of the flow response using the proposed high dynamic high voltage driver.
2) The settling time of the flow response using a low voltage driver.

Fig. 11 shows the flow step response of the servo-valve with a step value corresponding to the nominal flow for the Moog30 servo-valve $0.2 \times 10^{-3} m^3/s$, using the proposed high voltage driver, we observe that the settling time is $3.3ms$.

For the sake of better comparison, we placed the flow step response with the same condition just after in Fig. 12, where we can observe a $6ms$ of settling time, which means that the high voltage driver enhances the flow control loop speed by 181%.

To illustrate the high impact of the current driver we plotted the reference current (demanded by the PID controller) and the actual servo-valve current to examine the tracking in the current control loop. (Figure 13 and 14).

We can notice the poor tracking in case of low voltage current driver.

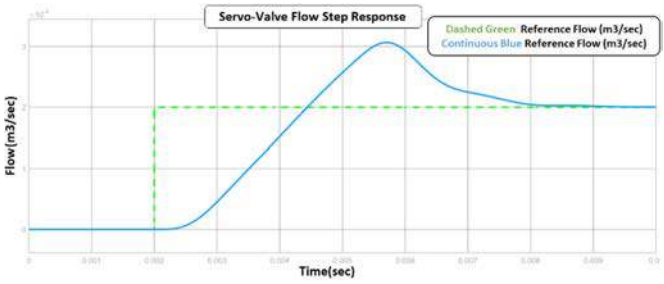

Fig. 12. Servo-valve Flow Step Response with High Dynamic Current

V. Implementation and Experimental Results

To test the driver, we implement the hydraulic circuit as shown in Fig. 9. In order to observe the enhancement in the current dynamics, the results of our driver are compared to two other drivers:

1) Off the shelf industrial driver My-502.
2) Developed H-bridge-based topology driver.

A. Experimental results

First, the current response of the servo-valve is measured using the industrial driver My-502, and it is shown in Fig 17 that the response represents $\pm 5mA$. The measured settling time is $T_{My-502_s} = 5ms = 0.5 \times T_{Torque_s}$.

Second, the H-bridge topology-based driver with digital PID implementation is tested, and we got the current step response

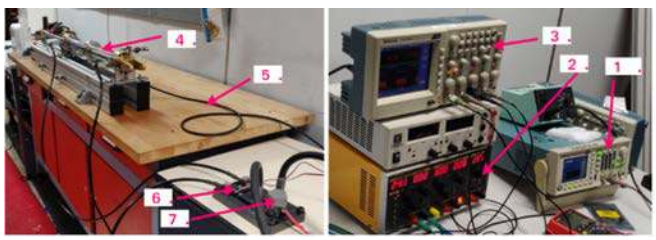

Fig. 15. Experimental Test Bench (1-Function Generator 2- Power Supply 3-Scope 4-Hydraulic Cylinder 5- Position Sensor 6- Pressure Sensor 7- EHSV)

Fig. 16. Our Developed high-voltage dynamic driver

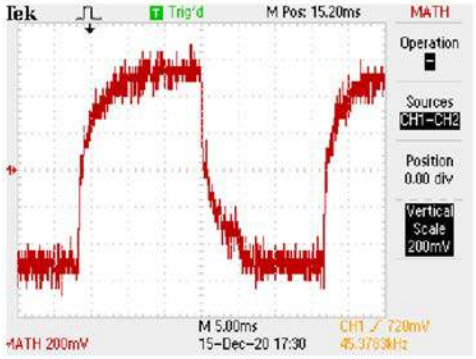

Fig. 17. Step response of the commercial driver MY-502

shown in Fig. 13 (the response represents $\pm 5mA$). The measurement of the current settling time gives $T_{Hbridge_s} = 2ms = 0.18 \times T_{Torque_s}$.

Finally, our proposed driver is tested under the same experimental conditions. The achieved step response is shown in Fig. 19.

The measured settling time, in this case, is $T_{HighDynamic_s} = 0.25ms = 0.02 \times T_{Torque_s}$. Our control has thus enhanced the settling time.

VI. Conclusion

This paper develops a driver that enhances the dynamics of the servo-valve system by making the current control faster and even permits controller designers to use whatever

Fig. 18. Step Response of H-Bridge-based Driver

Fig. 19. Step Response of Proposed Driver

model (4)-(5) because using such driver topology makes the knowledge of the current dynamics unnecessary.

Using the proposed driver in EHSV control system makes the current control loop fifty times faster than the flow outer loop. Moreover and since the servo-valve does not need a high driving current (in the milliamps range), there is no need to use the H-bridge Topology, and the high supply OP-AMPS is a very convenient approach for the driver design.

The proposed solution to drive the servo-valve based actuation system can be used for other actuators to enhance the dynamics, such as the SEHA actuator [24].

TABLE I.
Settling Time Drivers Comparison

Driver Type	**Current Settling Times** $[ms]$
My-502 Industrial Driver	$5ms = 50\% \times T_{Torque_s}$
H Bridge Topology	$2ms = 18\% \times T_{Torque_s}$
Proposed Op amp Driver	$0.25ms = 2\% \times T_{Torque_s}$

TABLE II.
MOOG30 Servo-valve parameters

Symbol	**Definition**	**Value for MOOG30 Servo-valve**
i	The current of Torque Motor	$\pm 10mA$
Q_v	Hydraulic Amplifier Differential flow	$\pm 4gpm$
X_s	Spool Displacement	$\pm 0.015in$
K_W	Feedback Wire Stiffness	$16.7in - lbs/in$
K_I	Torque Motor Gain	$0.025in - lbs/mA$
K_2	Hydraulic Amplifier Flow Gain	$150 \in^3 .sec^{-1}/in$
K_3	Flow Gain of Spool/Bushing	$1030 \frac{in^3.sec^{-1}}{in}$
K_f	Net Stiffness on Flapper/Armature	$115in - lbs/in$
A	Spool End Area	$0.026in^2$
ξ	Damping Ratio of the first Stage	0.4
ω_n	Natural Frequency of the first Stage	$814Hz$
L	Torque Motor Coil Inductance	$3.2H$
R	Torque Motor Coil Resistance	1000Ω

Acknowledgment

This work was supported by the PAUSE Program, KALYSTA, and SATT Paris-Saclay.

REFERENCES

[1] P. M. Wensing, A. Wang, S. Seok, D. Otten, J. Lang, and S. Kim, "Proprioceptive actuator design in the MIT Cheetah: Impact Mitigation and high-bandwidth physical interaction for Dynamic Legged Robots," IEEE Transactions on Robotics, vol. 33, no. 3, pp. 509–522, 2017.

[2] O. Stasse and T. Flayols, "An overview of Humanoid Robots Technologies," Springer Tracts in Advanced Robotics, pp. 281–310, 2018.

[3] T. Sugihara and M. Morisawa, "A survey: Dynamics of Humanoid Robots," Advanced Robotics, vol. 34, no. 21–22, pp. 1338–1352, 2020.

[4] F. Sygulla, R. Wittmann, P. Seiwald, T. Berninger, A.-C. Hildebrandt, D. Wahrmann, and D. Rixen, "An ethercat-based real-time Control System Architecture for Humanoid Robots," 2018 IEEE 14th International Conference on Automation Science and Engineering (CASE), 2018.

[5] R. Versluys, K. Deckers, M. Van Damme, R. Van Ham, G. Steenackers, P. Guillaume, and D. Lefeber, "A study on the bandwidth characteristics of pleated pneumatic artificial muscles," Applied Bionics and Biomechanics, vol. 6, no. 1, pp. 3–9, 2009.

[6] M. Ahmad Sharbafi, H. Shin, G. Zhao, K. Hosoda, and A. Seyfarth, "Electric-pneumatic actuator: A new muscle for Locomotion," Actuators, vol. 6, no. 4, p. 30, 2017.

[7] B. Vanderborght, B. Verrelst, R. Van Ham, M. Van Damme, and D. Lefeber, "A pneumatic biped: Experimental walking results and compliance adaptation experiments.," 5th IEEE-RAS International Conference on Humanoid Robots, 2005.

[8] G. Nelson, A. Saunders, and R. Playter, "The petman and Atlas Robots at Boston Dynamics," Humanoid Robotics: A Reference, pp. 169–186, 2018.

[9] G. Cheng, S.-H. Hyon, J. Morimoto, A. Ude, J. G. Hale, G. Colvin, W. Scroggin, and S. C. Jacobsen, "CB: A humanoid research platform for exploring neuroscience," Advanced Robotics, vol. 21, no. 10, pp. 1097–1114, 2007.

[10] B. UR REHMAN, M. FOCCHI, M. FRIGERIO, J. GOLDSMITH, D. G. CALDWELL, and C. SEMINI, "Design of a hydraulically actuated arm for a quadruped robot," Assistive Robotics, 2015.

[11] I did not find it in the site

[12] J. Yang, "Design and experiment of the lower extremity exoskeleton," 2017 IEEE 2nd Advanced Information Technology, Electronic and Automation Control Conference (IAEAC), 2017.

[13] C. Semini, N. G. Tsagarakis, E. Guglielmino, M. Focchi, F. Cannella, and D. G. Caldwell, "Design of hyq – a hydraulically and electrically actuated quadruped robot," Proceedings of the Institution of Mechanical Engineers, Part I: Journal of Systems and Control Engineering, vol. 225, no. 6, pp. 831–849, 2011.

[14] B. K. Sarkar, J. Das, R. Saha, S. Mookherjee, and D. Sanyal, "Approaching servoclass tracking performance by a proportional valvecontrolled system," IEEE/ASME Transactions on Mechatronics, vol. 18, no. 4, pp. 1425–1430, 2013.

[15] P. Xuan Hong Son and T. Thien Phuc, "Comparison of jet pipe servo valve with flapper nozzle servo valve," Science and Technology Development Journal, vol. 20, no. K1, pp. 78–83, 2017.

[16] P. Tamburrano, F. Sciatti, A. R. Plummer, E. Distaso, P. De Palma, and R. Amirante, "A review of novel architectures of Servovalves driven by piezoelectric actuators," Energies, vol. 14, no. 16, p. 4858, 2021.

[17] Y. Bai and L. Quan, "New method to improve dynamic stiffness of electro-hydraulic servo systems," Chinese Journal of Mechanical Engineering, vol. 26, no. 5, pp. 997–1005, 2013.

[18] S. Li and Y. Song, "Dynamic response of a hydraulic servo-valve torque motor with magnetic fluids," Mechatronics, vol. 17, no. 8, pp. 442–447, 2007.

[19] N. D. Manring and R. C. Fales, Hydraulic Control Systems. Hoboken, NJ: Wiley, 2020.

[20] Xu, Y. "Modelling and Control of a High Performance Electro-Hydraulic Test Bench". HAL. INSA de Lyon 2013.

[21] Y. Xu, E. Bideaux, and S. Sesmat, "Bond graph model of the intermediate block in a hydraulic control system," Proceedings of 2011 International Conference on Fluid Power and Mechatronics, 2011.

[22] Type 30 nozzle-flapper flow control servo valves. Available: https://www.moog.com/content/dam/moog/literature/sdg/defense/Moog-Type30-Servo-Valve-Catalog.pdf.

[23] 30 series micro servo valves. Available: https://www.moog.com/content/dam/moog/literature/products/servovalves/industrial/flow-control/analog/Moog-ServoValves-30Series-Datasheet-en.pdf.

[24] S. Alfayad, M. Kardofaki, and M. Sleiman, " Hydraulic Actuator with Overpressure Compensation." WO Patent No. 2020173933. International goffice 2020.